Id.: EN03

NEUTRONIC EVALUATION OF ADVANCED FUELS FOR SYSTEM-INTEGRATED MODULAR ADVANCED REACTOR (SMART)

Douglas S. Oliveira[1], Carlos E. V. Cabrera[1], Claubia Pereira[1], Clarysson A. M. Silva[1]
[1]Departamento de Engenharia Nuclear, Universidade Federal de Minas Gerais
(Av. Antônio Carlos, 6627, Campus UFMG, PCA 1, Bloco 04, Anexo Engenharia, Pampulha, 31270-90 Belo Horizonte, MG, Brazil)
douglasilva.olv@gmail.com

Key words: Neutronic Analysis, Monte Carlo Method, Small Modular Reactor, SMART.

ABSTRACT

In contemporary society, energy production stands as a crucial focal point, driven by humanity's heavy reliance on energy sources. However, the pressing concerns regarding environmental ramifications associated with energy generation, especially in the context of global warming and climate change, have taken center stage. Consequently, numerous nations are actively pursuing carbon-neutral energy solutions and investing in pioneering technologies. Among these solutions, nuclear energy emerges as a promising carbon-zero source, with innovations like Small Modular Reactors (SMRs) gaining prominence due to their potential to complement intermittent renewable energy sources. SMRs, exemplified by the SMART reactor developed by KAERI, offer streamlined systems and quicker construction compared to conventional nuclear plants. SMART serves multiple purposes including electricity generation, heating, desalination, and industrial process heat. Its advanced design has undergone thorough safety and performance testing, affirming its reliability. In conjunction with small modular reactors (SMRs), significant advancements have been made in the development of advanced fuels over recent decades. These fuels possess characteristics capable of addressing existing deficiencies and enabling the creation of more economically viable nuclear systems equipped with inherently designed safety features. These materials offer enhanced safety and improved economics for nuclear reactors, allowing for longer operational lifespans under higher levels of neutron irradiation. Moreover, they enable higher operating temperatures and exhibit greater resistance to aggressive corrosive environments, thereby enhancing overall reactor performance and durability. Even the predominant fuel utilized in light water reactor (LWR) systems is Uranium Dioxide (UO_2), there is a notable increase in research investments directed towards exploring alternative fuels. Notably, Uranium Mononitride (UN) and Uranium Carbide (UC) offer advantages such as increased burnup capabilities and higher thermal conductivities, while Uranium Silicide (U_3Si_2) demonstrates superior resistance to Reactivity-Initiated Accidents (RIAs). This study delves into an evaluation of the neutronic behavior of SMART reactor under different fuel configurations, using UO_2, UN, UC, and $U3Si_2$ with similar enrichment levels. By analyzing various neutronic parameters, our aim is to offer comprehensive insights into the efficacy and safety of different fuels for energy generation in SMRs. This research endeavor seeks to elucidate the impact of fuel variations on neutron parameters, thereby providing valuable guidance for future reactor design and operational considerations in the context of SMRs.

1. INTRODUCTION

Small Modular Reactors (SMRs) are a way of generating energy from nuclear sources, with advantages over traditional nuclear power plants, offering low initial investments, a reduced construction area and the possibility of reactor mobility, since the core is reduced in size and can be transported by truck, for example. Nowadays, the SMRs are being considered as an alternative to complement intermittent renewable energy sources. The System Integrated Modular Advanced Reactor (SMART), developed by the Korea Atomic Energy Research Institute (KAERI) [1], represents a significant advancement in the SMRs field, given that the SMART, an integral Pressurized Water Reactor (PWR), incorporates advanced design features

to enhance safety, reliability, and economics. The goal for this reactor is to optimize economics by simplifying the system, modularizing components, reducing construction time, and ensuring high plant availability. Along with that, there has been growing investment in research and development in the area of advanced fuels, an expanding field that complements the nuclear energy sector. The configuration and composition of the fuel play a fundamental role in nuclear power generation, which has led to extensive research into materials to introduce new types of fuel with the main aim of increasing efficiency and safety. As elucidated by D. Yun paper [2], These advanced fuels have interesting attributes that can contribute to reducing some existing deficiencies and, consequently, facilitate the development of more economically viable nuclear systems, while maintaining the safety features required for nuclear generation. These materials offer higher safety standards and greater economic viability for nuclear reactors, allowing for an extended operational lifespan, even under high levels of neutron irradiation. Furthermore, they exhibit enhanced thermal stability, enabling operation at higher temperatures, and demonstrate superior resilience to corrosive environments, thus increasing overall reactor performance and longevity of the reactor. In this context, the present paper evaluates the use of advanced fuels in SMART comparing Uranium Mononitride (UN), Uranium Carbide (UC) and Uranium Silicide (U_3Si_2) with conventional Uranium Dioxide (UO_2). This study aims to determinate the main neutronic parameters of the reactor to verify the applicability of advanced fuels in SMART. The work uses Monte Carlo N-Particle code – version 6.2 (MCNP6.2) for the calculations.

2. METHODOLOGY

2.1 Main Characteristics of the Simulated Reactor

The SMART reactor, developed by KAERI, features a core area of 2.64 m² and a core diameter of 183.2 cm. Comprising 57 fuel assemblies; each assembly houses 264 fuel rods, each with a diameter of 8.05 mm and a height of 2.0 m [3]. There are four types of fuel assemblies (A, B, C and D) and each one has a specific configuration, with a unique number and arrangement of rods, as illustrated in Fig. 1.

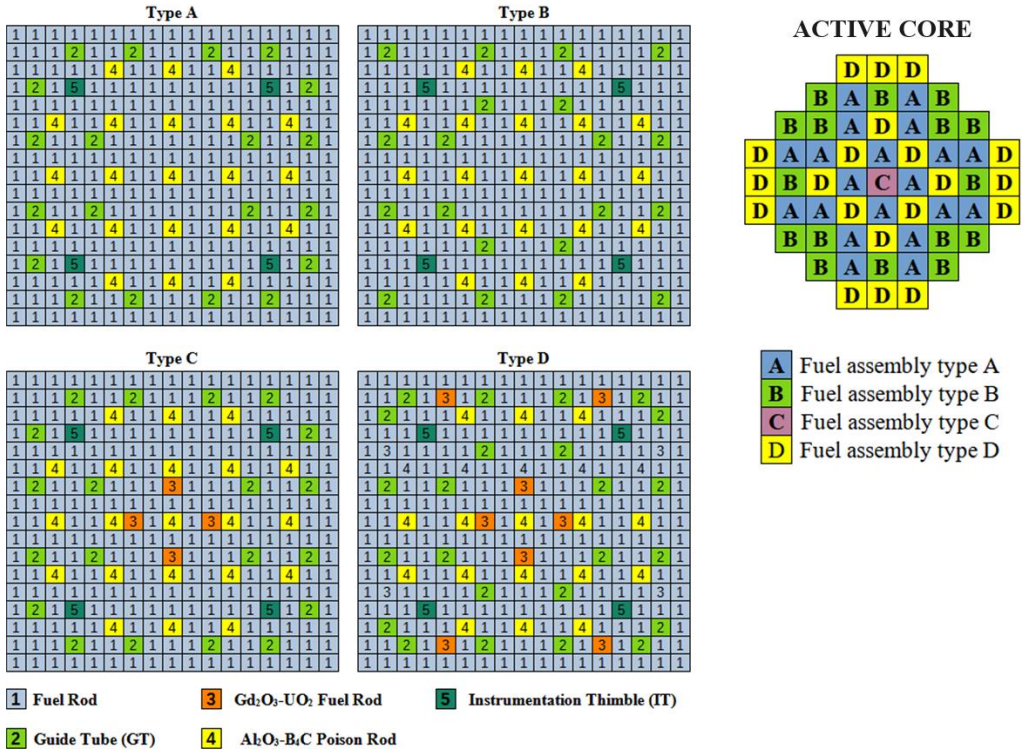

Fig. 1. Fuel configuration for the SMART [3].

The enrichment of the uranium dioxide fuel is at 4.95% and the reactor achieves a thermal capacity of 330 MWt (mega-watt thermal) at a nominal operating temperature of 750 Kelvin. In addition, Fig. 1 depicts the core-loading pattern for the first reactor cycle showing the arrangement of the different fuel types of fuel assemblies present in the SMART reactor core. The present study simulates the UO_2 fuel proposed by KAERI and compares it with the advanced fuels UN, UC, and U_3Si_2, considering the same fuel enrichment of 4.95% of ^{235}U and a similar configuration. The Tab. 1 presents the fuel density and the fuel temperature of the simulations.

Tab. 1. Main data of simulated fuels

Parameter	**UO_2**	**UN**	**UC**	**U_3Si_2**
Density ($g \cdot cm^{-3}$)	10.41	13.59	12.95	11.59
Temperature (K)	750	750	750	750

Monte Carlo (MC) codes have been widely used around the world to simulate the neutronic behavior of various nuclear reactors. MCNP is one of the primary Monte Carlo codes used to analyze steady-state neutronic parameters such as the multiplication factor, neutron flux, reaction rates, and other reactor physics constants. The steady-state analyses are performed using particle transport calculus with the MC method. This technique plays a significant role in performing neutronic calculations accounting for the spatial dependence of neutron flux in three-dimensional geometry.

The MCNP6.2 model comprises a 3D geometry configured according to the core characteristics described before. This model considers the isotopic composition and density corresponding to the first cycle of SMART [2]. The results were obtained from comprehensive full-core calculations, simulating 100 active cycles with 70,000 neutrons per cycle. To ensure the

convergence of the fission source distribution, each simulation excluded 15 inactive cycles before initiating active tallies. The simulations use ENDF-B/VII library data [4].

2.2 Evaluated Parameters

The studied fuels have different compositions and densities, and thus they provoke different reactivity excess (ρ_{ex}) in the SMART core. To evaluate this parameter, the traditional equation was used, as presented in the book by Lamarsh and colleagues [5]:

$$\rho_{ex}(pcm) = \left(\frac{k_{eff} - 1}{k_{eff}}\right) \cdot 10^5 \tag{1}$$

where k_{eff} is the effective multiplication factor calculated by the MCNP6. Also, among several parameters, this code calculates the average number of neutrons emitted per fission (ν), the neutron reproduction factor (η) and the prompt neutron lifetime (l_p). However, some parameters such as the effective delayed neutron fraction (β_{eff}) are not calculated directly by MCNP6. The usual method to calculate it is:

$$\beta_{eff} = 1 - \frac{k_p}{k_{eff}} \tag{2}$$

where k_p is the effective multiplication factor of the system considering only prompt neutrons. Now, distinct fuels may generate different l_p and β_{eff} values, resulting in different reactor period (T), expressed by:

$$T = \frac{l_m}{k_{eff} - 1} = \frac{\left(1 - \beta_{eff}\right) \cdot l_p + \beta_{eff} \cdot l_d}{k_{eff} - 1} \tag{3}$$

where l_d is the delayed neutron lifetime. These differences are critical for reactor control and safety analysis, necessitating careful consideration of fuel type in reactor design and operation. Thus, to evaluate a power transient from P_0 to P following a change in a critical system, the traditional equation was used:

$$P = P_0 \cdot \exp\left(\frac{t}{T}\right) \tag{4}$$

where t is the transient time. The present study considers t = 1.0 s and l_d = 12.7 s for all cases.

Furthermore, recalling that the reproduction factor can be calculated as (taken from [5]):

$$\eta = \nu \cdot \frac{\Sigma_f}{\Sigma_a} \tag{5}$$

where Σ_f and Σ_a are the respective macroscopic cross section for fission and absorption reactions in the fuel, the fission probability (FP) can be calculated as:

$$FP = \frac{\eta}{\nu} = \frac{\Sigma_f}{\Sigma_a} \tag{6}$$

As SMART uses light water as both coolant and moderator, any density changes may affect the core's reactivity [6]. In this sense, the Coolant Void Coefficient (CVC) is an important parameter in reactor safety analysis because it describes the change in reactivity as a function of voids or absence of coolant in the reactor core. This parameter helps assess the stability and safety margins of the reactor under various operational conditions, including possible accidents or operational transients. In the simulations, the CVC was calculated as (based on the definition presented in [6]):

$$CVC(pcm) = \frac{\Delta\rho}{VF} \cdot 10^5 = \left(\frac{1}{k_{ST}} - \frac{1}{k_{PT}}\right) \cdot \frac{1}{VF} \cdot 10^5 \quad (7)$$

where k_{ST} and k_{PT} are the k_{eff} values calculated at standard (*ST*) and perturbed (*PT*) coolant condition respectively, for a specific coolant void fraction (*VF*). The simulations explore two scenarios for CVC calculations: the first calculates *VF* by varying the coolant density (*d*), and the second calculates *VF* by varying the coolant volume (*V*) as:

$$VF = \frac{d_{ST} - d_{PT}}{d_{ST}} \qquad \text{and} \qquad VF = \frac{V_{ST} - V_{PT}}{V_{ST}} \quad (8)$$

where d_{ST}, d_{PT}, V_{ST}, and V_{PT} are the respective values of density and volume at standard (*ST*) and perturbed (*PT*) coolant conditions. The first scenario simulates the reactor core fully immersed in water, varying the coolant density from 0% to 100%. In the second case, the nominal coolant density is maintained, but the water level in the core is decreased, thereby reducing the coolant volume to simulate a Loss of Coolant Accident (LOCA).

About the neutron flux, the absolute values calculated by MCNP6 do not match the actual neutron source of the reactor. Thus, the flux normalization was performed as shown below, as defined in the report by J.T. Goorley [7]:

$$\varphi_N = \varphi_{MCNP6} \cdot \left(\frac{P \cdot \nu}{Q \cdot k_{eff}}\right) \quad (9)$$

where φ_N is the normalized flux; φ_{MCNP6} is the flux estimated by MCNP6; *P* is the reactor power (330 MW) and is the recoverable energy per fission event. For assessing the neutron energy spectrum, the neutron flux was calculated considering the total core volume, which includes the active core and the reflector region. In this case, the neutron energy was discretized from 10^{-9} to 10^{1} MeV.

3. RESULTS AND DISCUSSION

Tab. 2 presents the criticality and reactivity of SMART with all control rods, which contains burnable poison composed of Al_2O_3-B_4C with enriched boron with 30% of ^{10}B, with the fully removed. In this core condition, all cases provoke a supercritical core condition, as expected. The standard deviations of the k_{eff} are on the order of 80 pcm.

Tab. 2. Neutronic parameters at Beginning of Cycle for SMART.

Parameter	**UO_2**	**UN**	**UC**	**U_3Si_2**
k_{eff}	1.07476	1.05708	1.11455	1.09549
ρ_{ex} (pcm)	6956	5400	10278	8717
FP	0.43701	0.42913	0.45226	0.44506

The behavior of k_{eff} and ρ_{ex} agree with the Fission Probability (*FP*) calculated by Equation (6). Surely, higher *FP* tends to lead to higher values of k_{eff} and ρ_{ex}. Then, among the fuels, UC has the highest values while UN has the smallest. This behavior may be due the different fuel densities and the distinct cross-sections of oxygen, nitrogen, carbon and silicon. Alongside with that, Fig. 1 depicts the microscopic cross-sections for capture reactions of the main isotopes of these elements. It is noticeable that ^{14}N has the highest values among the nuclides. Also, UN has the highest fuel density (as shown in Tab. 1) and therefore, the highest concentration of absorber ^{238}U. Consequently, this fuel has the smallest criticality among the cases.

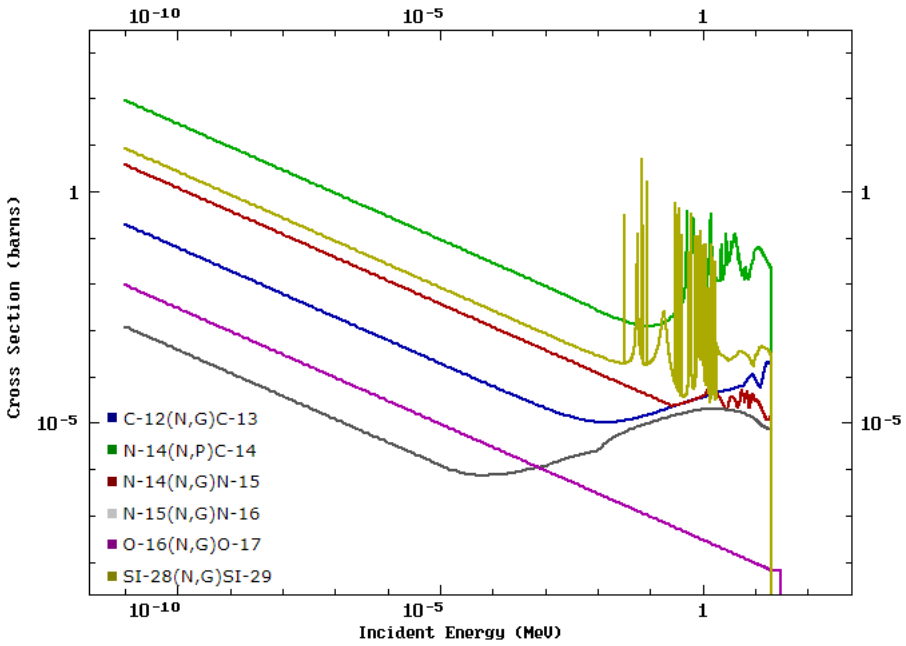

Fig. 2. Fuel configuration for the SMART. Image adapted from [3] by the authors.

Fig. 3 illustrates the neutron energy spectrum of the SMART core for the evaluated cases. The spectrum profiles are similar for the fuels, with the biggest difference in the thermal energy range. This difference affects the percentage of fissions in the thermal energy range, which increases as the thermal neutron flux increases (as shown in Tab. 3). In this energy interval, UO_2 has the highest neutron flux, while UN has the smallest. Consequently, UO_2 has the highest percentage of fissions in the thermal range, whereas UN has the smallest (according to Tab. 3). This behavior may be due to the highest capture cross-section of ^{14}N (based on the result presented in Fig. 2). Furthermore, UN has the highest percentage of fission in epithermal and fast energy range (as shown in Tab. 3). The highest fuel density of UN may be contributing to a highest fast fission due the highest ^{238}U concentration.

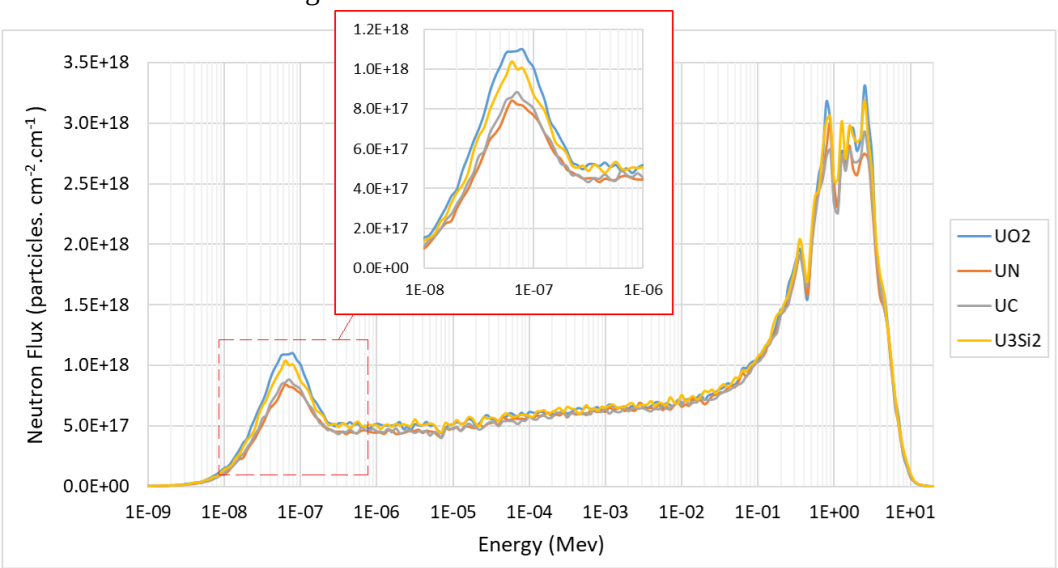

Fig. 3. Results of simulations in MCNP6 for Energy Spectrum.

Tab. 3. Percentage of fissions caused by neutrons in different neutron energy ranges.

Energy Range		**UO_2**	**UN**	**UC**	**U_3Si_2**
Thermal	< 0.625 eV	79.80%	73.94%	75.54%	77.59%
Epithermal	0.625 eV – 100 keV	14.08%	18.00%	16.96%	15.51%
Fast	> 100 keV	6.12%	8.07%	7.50%	6.90%

As UO_2, UN, UC and, U_3Si_2 provoke different reactivity excesses (according to Tab. 2), the action of the control rods generates distinct variations in reactor power. Tab. 4 presents the reactivity variation between two control rod positions: fully removed and scram conditions. The UO_2 has the highest negative reactivity insertion while the UN has the smallest. UN has a harder neutron spectrum than UO_2 (as shown in Fig. 3), and so radiative capture reactions in control rods are smaller for UN when compared to UO_2.

Tab. 4. Negative reactivity insertion to total insertion of control rods.

Control Rods Condition	**Insertion Depth (cm)**	**UO_2**	**UN**	**UC**	**U_3Si_2**
Fully Removed	0.0	6956	5400	10278	8717
Scram	300.0	-14209	-13080	-8351	-11204
Reactivity variation		-21165	-18480	-18628	-19920

Furthermore, Fig. 4 illustrates the reactivity variation for different insertion depth of control rods. The evaluated fuels exhibit similar reactivity behavior, $\rho(x)$, as a function of the insertion depth of the control rods (Fig. 4a). All cases show the highest variation of $\rho(x)$ between 150 and 225 cm of insertion depth (Fig. 4b). Note that the curve profile in Fig. 4b supports the observation of spectrum hardening (Fig. 3). As the neutron spectrum becomes harder, the fractional rate of reactivity change decreases, which is expected of a reactor under these conditions. Again, UO_2 shows the highest change, while UN shows the smallest.

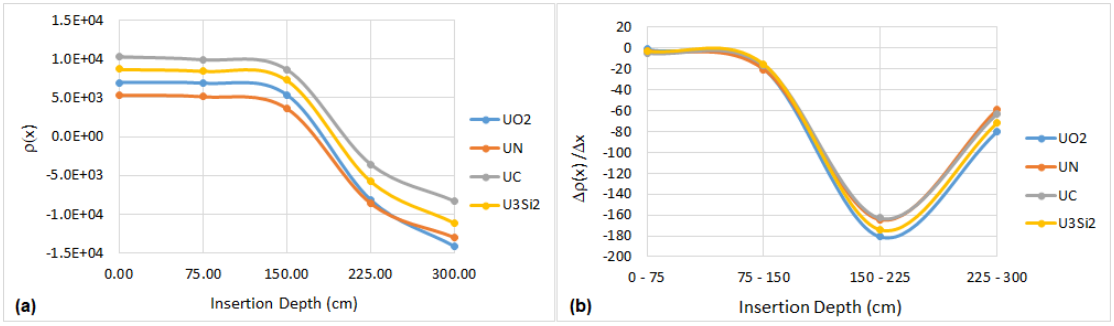

Fig. 4. (a) Control rod worth as a function of their insertion depth; (b) Fractional rate of reactivity change per unity of insertion depth.

Tab. 5 presents the l_p and β_{eff} calculated by MCNP6 for studied fuels. Thus, considering a criticality increase of 100 pcm from a critical system (k_{eff} = 1.001) and an initial power (P_0) equal to 33% of the total SMART power, the reactor period (T) during a power transient was calculated using Equations (3) and (4). As described in the literature, β_{eff} is an important factor in this transient analysis, where a higher β_{eff} results in a higher T and a smaller P/P_0. Among the cases, UO_2 shows the highest power increase at 1.4%, while UC shows the smallest at 1.0%. To choose the most suitable fuel in this case, UC would be more appropriate, as it has a smaller increase in power, since a very large increase each cycle could be difficult to control.

Tab. 5. Kinetic parameters for evaluated fuels

Fuel	l_p (μs)	β_{eff} (pcm)	k_{eff}	T (s)	P_0 (MW)	P (MW)	P / P_0
UO_2	20.6	584	1.001	73.7	100.0	101.4	1.014

UN	16.5	607		77.5	100.0	101.3	1.013
UC	17.3	792		100.3	100.0	101.0	1.010
U_3Si_2	18.9	676		85.1	100.0	101.2	1.012

Tab. 6 presents the CVC calculated using Equations (7) and (8) for the two scenarios involving variations in coolant density (*d*) and coolant volume (*V*). Most cases exhibit negative values, indicating that an increase in void fraction (*VF*) leads to a reduction in k_{eff}, which corresponds to a decrease in fission reactions. This behavior is a desirable safety feature because it conduces to a reactivity reduction and shut down the reactor in the event of a coolant density reduction and/or LOCA. However, UC and U_3Si_2 have positive CVC values for a specific range of VF variation. Uranium carbide has a CVC of 78 pcm for VF = 40–50% in the coolant density variation scenario. Uranium silicide has a CVC of 12 pcm for VF = 10–20% in the LOCA scenario. In these specific situations, reactivity might increase, potentially resulting in unsafe conditions. However, the standard deviation of k_{eff} is about 80 pcm, and some CVC values may be statistically equal.

Tab. 6. Coolant Void Coefficient for different scenarios of reactor core.

VF	**Coolant Density Variation**				**Coolant Volume Variation (LOCA)**			
	UO_2	**UC**	**UN**	**U_3Si_2**	**UO_2**	**UC**	**UN**	**U_3Si_2**
0 – 10 %	-173	-24	-40	-30	0	0	0	0
10 – 20 %	-150	-34	-14	-6	0	0	0	12
20 – 30 %	-174	-20	-34	-49	0	-10	-41	-15
30 – 40 %	-438	-125	-28	-22	-43	-48	-7	-49
40 – 50 %	-650	78	-71	-55	-67	-68	-77	-74
50 – 60 %	-973	-94	-29	-59	-227	-152	-138	-161
60 – 70 %	-1519	-74	-95	-53	-377	-374	-407	-446
70 – 80 %	-2674	-45	-83	-98	-1789	-1682	-1667	-1836
80 – 90 %	-11261	-137	-175	-122	-19026	-16699	-17021	-18251
90 – 100 %	-12666	-207	-283	-308	-86299	-64683	-62553	-79222

4. CONCLUSION

This paper studies the use of UN, UC, and U_3Si_2 in a small modular reactor of PWR type, comparing them with traditional UO_2. Among the evaluated fuels, UN produces the smallest core reactivity, while UC produces the highest, with an increase of 3322 pcm compared to traditional UO_2. Then, the UC has smaller control rod worth than UO_2. Additionally, UC has the highest β_{eff}, which provides better control during reactivity transient. Regarding the CVC, most fuels present negative values, but it is important to evaluate this parameter by running MCNP6 with a higher number of particle histories to decrease the standard deviation and assess the uncertainty of the CVC. The uncertainty propagation of CVC calculation will be performed in future studies Furthermore, since UC and U_3Si_2 have higher k_{eff} than UO_2, they may contribute to an extended burnup in the reactor cycle. Thus, upcoming research will evaluate the evolution of fuel during the reactor cycle, aiming to study the neutronic parameters and the fuel composition of SMART throughout the cycle.

Considering that the present work focuses on neutronic studies, undoubtedly, further studies in distinct fields such as thermal-hydraulic, metallurgy, reactor shielding, among others, will be needed for the implementation of UN, UC, and U_3Si_2. For the possible use of these fuels in SMRs, it will be necessary to carry out further analyses related to other reactor parameters. The present work is in development and may serve as a basis for these analyses.

ACKNOWLEDGMENTS

The authors are grateful to the following Brazilian research funding agencies: FAPEMIG (Fundação de Amparo à Pesquisa do Estado de Minas Gerais), CAPES (Coordenação de Aperfeiçoamento de Pessoal de Nível Superior), CNPq (Conselho Nacional de Desenvolvimento Científico e Tecnológico), and CNEN (Comissão Nacional de Energia Nuclear).

REFERENCES

[1] Kang O. H. et al. (2024). Light water SMR development status in Korea. Nuclear Engineering and Design, Volume 419, 112966. ISSN 0029-5493. DOI: 10.1016/j.nucengdes.2024.112966.

[2] Yun, D., et al. (2021). Current state and prospect on the development of advanced nuclear fuel system materials: A review. Materials Reports: Energy, 1(1), 100007. Available online at: https://doi.org/10.1016/j.matre.2021.01.002. Accessed on April 03, 2024.

[3] Park, S. Y., et al. Nuclear Characteristics Analysis Report for System-integrated Modular Advanced Reactor. Korea: Korea Atomic Energy Research Institute, 1998.

[4] National Nuclear Data Center. ENDF/B-VII.1: Evaluated Nuclear Data File. 2011. Disponível em: https://www.nndc.bnl.gov/endf-b7.1/. Acesso em: 24 jul. 2024.

[5] Lamarsh, J. R.; Baratta, A. J. Introduction to Nuclear Engineering. [S.l.]: Prentice Hall, 2001.

[6] Cardoso, E. de M. Educational Handbook on Nuclear Energy. Rio de Janeiro: National Commission of Nuclear Energy, 2013.

[7] Goorley, J.T et al 2013. Initial MCNP6 Release Overview - MCNP6 version 1.0. Los Alamos National Laboratory. Report LA-UR-13-22934 (USA).

[8] Peixoto, S. M. de et al. Neutronic simulation of the TRIGA nuclear research reactor at CDTN using the Monte Carlo Serpent and MCNPX codes. Revista Tecnologia, Belo Horizonte, 2004.